Energy Bands in Body-Centered and Hexagonal Sodium*

A. James Hughes† and Joseph Callaway
Department of Physics, University of California, Riverside, California
(Received 2 July 1964)

The band structures of both the body-centered cubic and the hexagonal close-packed phases of sodium have been computed using a pseudopotential method. The pseudopotential parameters were obtained from spectroscopic data for the free sodium atom. The Fermi surface is nearly spherical in both phases, with the maximum distortion being of the order of $\frac{1}{4}\%$. Within the accuracy of the calculation, the Fermi energy and effective mass are the same in the two phases.

INTRODUCTION

ALTHOUGH many energy-band calculations have been performed for sodium,[1] comparison of calculated energy bands with experiment has been complicated by the low-temperature martensitic phase transformation. Samples at low temperatures contain both body-centered cubic and hexagonal close-packed phases. In order to study the effect of the presence of the hexagonal phase of sodium on experiments concerning the band structure, we have calculated energy bands for both the body-centered cubic and the hexagonal close-packed phases. A form of the pseudopotential method has been employed in which the parameters of the potential are determined from free-atom spectroscopic data. Since the same pseudopotential is used for both phases of sodium and since the calculations employ essentially the same number of plane waves for both phases, differences between the calculated energy bands in the two phases may be ascribed to the difference in crystal structure.

We conclude that the energy-band structure for the two phases are essentially the same. Within the accuracy of the band calculations we have obtained the same effective mass and the same Fermi energy for both phases. A single effective mass is therefore to be expected from samples of sodium containing amounts of both crystal phases.

Our procedures may be summarized briefly as follows. The wave function for each state is expanded in terms of symmetrized combinations of ordinary plane waves. A repulsive pseudopotential is used which incorporates the effects due to orthogonality of the valence electrons to the wave functions of the core electrons. The parameters of the repulsive pseudopotential are determined from spectroscopic data for the free atom. For the present problem which deals with the change in crystal structure between the two phases of sodium, the plane-wave method has the advantage that the potential can be evaluated in a manner consistent with the full symmetry of the crystal lattice more easily than in most other methods. In our calculations for the hexagonal phase, we have ignored the presence of stacking faults, and have employed the double-zone scheme. The use of the double-zone scheme should be appropriate either when spin-orbit effects are small or when magnetic breakdown has occurred.

THE PSEUDOPOTENTIAL

The present application of the pseudopotential method to determine an explicit potential suitable for energy-band calculations is based upon arguments similar to those used in the development of the quantum defect method (QDM).[2] These arguments have been presented in detail elsewhere.[1,3] The basic assumption is that for the calculation of wave functions and valence-electron energies, we may take as our one-electron Hamiltonian an operator which near an ion in the solid is the same as in the free atom. The development of the QDM indicates that detailed information concerning the form of the potential inside the core region is not necessary in order to compute energy levels of valence electrons in the solid provided the potential is Coulombic near the cell boundary. In the region where the potential is Coulombic, the wave function is a linear combination of the regular and irregular solutions of the Coulomb wave equation. The ratio of the coefficients in this combination is a function of energy which can be determined for energies corresponding to eigenvalues of the free atom, and extrapolated to other energies. Once the ratio is known, the wave function on the cell boundary is determined to within a multiplicative factor, and consequently the energies at which the various states ψ_k satisfy the appropriate boundary conditions can be determined.

For the present calculation we desire an explicit potential which meets the general requirements of the QDM and in addition incorporates the effects of orthogonality so that ordinary plane waves can be used conveniently. For our potential we may therefore use any function which is Coulombic outside the core, reproduces the free-atom eigenvalues correctly, and therefore yields the correct logarithmic derivatives in the exterior region at these eigenvalues. A pseudopotential which meets these requirements is assumed

* Supported by the U. S. Air Force Office of Scientific Research.
† Present address: Research Laboratory, Philco Corporation, Newport Beach, California.
[1] Energy band calculations for the alkali metals have been reviewed by J. Callaway, *Energy Band Theory* (Academic Press Inc., New York, 1964), Chap. 3.
[2] F. S. Ham, in *Solid State Physics*, edited by F. Seitz and D. Turnbull (Academic Press, Inc., New York, 1955), Vol. 1, p. 127.
[3] J. Callaway, Phys. Rev. 112, 322 (1958).

to be a satisfactory potential for the energy-band calculation. In principle, the use of such a pseudopotential to yield a wave function with the desired logarithmic derivatives outside the core region does not introduce any approximations into the problem other than those connected with the general validity of the QDM. In practice, some additional approximations are introduced because the pseudopotential contains only a few parameters.

For the pseudopotential we use a form introduced by Hellmann and Kassatotschkin[4] and applied to sodium by Callaway[3]

$$V(r)=-2/r+Qe^{-Br}/r. \quad (1)$$

It is necessary that the parameter B be large enough so that a small core is simulated and so that there is a well-defined region in which the potential is Coulombic.

It must be expected that different values for the parameters of the pseudopotential will be obtained depending on the states used to determine them. The effect of exchange can be considered to a good approximation as giving rise to a different potential for states of different angular momentum.[5] In some cases it might be desirable to determine a pseudopotential for each angular momentum. However, the difference of the effective exchange potential between the different angular-momentum states is likely to produce only a small effect in sodium as is evidenced by the success of Prokofjew in accounting for all the spectral levels on the basis of a single potential.[6] We have therefore determined a single pseudopotential based on the $3s$ and $3p$ states.

In order to determine the parameters of the pseudopotential, the following procedure was adopted. For the form of the pseudopotential we have used, the radial Schrödinger equation is given by

$$(d^2R_L/dr^2)+[E_{n,L}+2/r-Qe^{-Br}/r -L(L+1)/r^2]R_L=0, \quad (2)$$

where $E_{n,L}$ is the experimental eigenvalue for the free-atom state in question and Q and B are trial values of the pseudopotential parameters. For a particular state, say the $3s$ state, the radial equation is integrated numerically from the origin outward into the Coulombic region. For a value of r in the Coulombic region, the trial value of the logarithmic derivative is calculated. The values of the logarithmic derivatives so obtained were then compared with values of the derivatives required if R_L is to be an eigenfunction. The parameters Q and B were varied until reasonable agreement was obtained.

The values of the logarithmic derivatives of the free-atom eigenfunctions were determined from an asymptotic series for the wave function using the experimental eigenvalues. This series is described in Ref. 3. For each of the states $3s$, $3p$, $4s$, and $4p$, curves of the pairs of values Q and B which yield correct logarithmic derivatives were obtained. Each of these curves represents the locus of points Q and B for which the correct logarithmic derivative is obtained. A potential may be determined from the intersection of any two of the potential curves. The (Q,B) region which was investigated by this method was $10\leq Q\leq 45$ and $1.5\leq B\leq 2.5$. The intersections which were found are given in Table I. The intersection of the $3s$ and $3p$ potential curves determined the potential we believe appropriate for the energy-band problem. The values of the parameters Q and B were therefore taken to be $Q=20.3$ and $B=2.044$. Using this pseudopotential, it was found that the $3s$ free-atom eigenvalue was reproduced correctly to within 1.2%, and the $3p$ eigenvalue was correctly reproduced to within 0.8%.

TABLE I. Four determinations of the pseudopotential parameters for the free atom.

States	Q	B
$3s-3p$	20.3	2.044
$4s-4p$	24.3	2.12
$3s-4p$	13.6	1.77
$4s-3p$	30.4	2.26

Although the $3s-3p$ pseudopotential has been used in the energy-band calculation, the energy of the ground state Γ_1 for the body-centered cubic lattice was calculated for the four different pseudopotentials we have obtained in order to determine the sensitivity of the Γ_1 state to changes in the pseudopotential parameters. The results obtained are given in Table II and are for an equivalent sphere radius of 3.96 a.u. (atomic units). The energy is given in rydbergs and the usual cellular zero of energy is taken. Apparently the energy of the state Γ_1 is not very sensitive to the particular potential used as long as the derivatives are reproduced correctly.

THE BAND-STRUCTURE CALCULATION

The wave function for each of the two crystal structures is expanded in a linear combination of symmetrized groups of plane waves chosen to belong to a particular representation of the group of the wave

TABLE II. The energy of the ground state Γ_1 for bcc sodium for four different free atom pseudopotentials. The s-curve potential given below is from an arbitrary point on the (Q,B) curve along which the $3s$ logarithmic derivative is correctly reproduced.

Q	B	Pseudopotential	E (rydbergs)
28	2.26	s curve	−0.6049
24.3	2.12	$4s-4p$	−0.5988
20.3	2.044	$3s-3p$	−0.6031
13.6	1.77	$3s-4p$	−0.5984

[4] H. Hellmann and W. Kassatotschkin, J. Chem. Phys. 4, 324 (1936).
[5] F. Herman, J. Callaway, and F. S. Acton, Phys. Rev. 95, 371 (1954).
[6] W. Prokofjew, Z. Physik 58, 255 (1929).

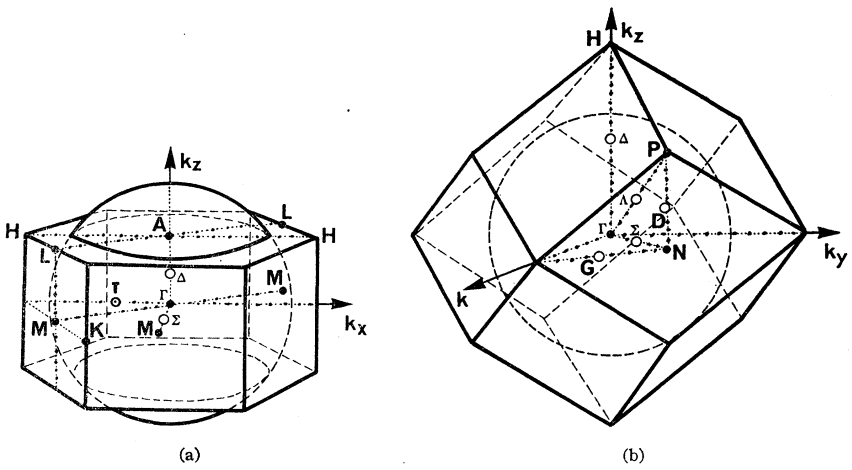

FIG. 1. The Brillouin zone and Fermi surface for (a) the close-packed hexagonal and for (b) the body-centered cubic phases of sodium.

vector. If $\psi_{\mathbf{k}}{}^{i}$ is the wave function for the ith irreducible representation of wave vector $\mathbf{k}$, one has

$$\psi_{\mathbf{k}}{}^{i}=(1/\Omega_0)^{-1/2}\sum_{\mathbf{h}} a_{\mathbf{k}+\mathbf{h}}{}^{i}\exp[i(\mathbf{k}+\mathbf{h})\cdot\mathbf{r}]. \quad (3)$$

The sum over $\mathbf{h}$ runs over all reciprocal lattice vectors for the lattice in question. For the present, we ignore the relations between the $a_{\mathbf{k}+\mathbf{h}}$ which are a consequence of symmetry. Ω_0 is the volume of the cellular polyhedron. The matrix elements of the Hamiltonian are

$$\langle\mathbf{k}+\mathbf{h}|H|\mathbf{k}+\mathbf{h}'\rangle=(\mathbf{k}+\mathbf{h})^2\delta_{\mathbf{h}\mathbf{h}'}+V(\mathbf{h}-\mathbf{h}'), \quad (4)$$

where the Fourier coefficients $V(\mathbf{h}-\mathbf{h}')$ are given by

$$V(\mathbf{h}-\mathbf{h}')=(1/\Omega_0)\int_0\exp[-i(\mathbf{h}-\mathbf{h}')\cdot\mathbf{r}]V(\mathbf{r})d^3r. \quad (5)$$

For the body-centered cubic lattice the above integral is over the cellular polyhedron containing one atom while the hexagonal structure is taken over the double polyhedron centered about the two atoms of the basis. The crystal potential we have used in the band calculation is that of Eq. (1) neutralized by a uniform distribution of negative charge within the cellular polyhedron. The Fourier coefficients $V(\mathbf{h}-\mathbf{h}')$ were computed with the full symmetry of the cellular polyhedron for the crystal structure in question. The determination of the Fourier coefficients of the potential is discussed at greater length in Appendix.

In the case of the cubic phase of sodium we have used the lattice constant quoted by Barrett[7] which is $a=4.225$ Å at 5°K. The corresponding equivalent sphere radius is 3.931 a.u. Unless specified to the contrary, results for the energy-band calculations refer to this sphere radius and pseudopotential parameters $Q=20.3$ and $B=2.044$. In order to investigate the dependence of the energies of the symmetry points Γ and N on these quantities, additional values of the sphere radius and pseudopotential parameters have been employed and are given where applicable.

[7] C. S. Barrett, Acta Cryst. **9**, 671 (1956).

The calculation for the cubic phase involved solving secular determinants for between 273 and 295 plane waves depending on the representation. The order of secular determinant varied from 15 for the Γ_1 state to 90 for the Σ_1 representation. Energies were determined for the Λ_1, Δ_1, and Σ_1 representations along the Λ, Δ, and Σ symmetry axes, and for the Γ_1, N_1, and N_1' representations at the symmetry points Γ and N. Only states of predominantly s and p symmetry were treated since for states of predominantly d (or higher l) symmetry, the pseudopotential approach cannot be used because sodium lacks a core function of like symmetry. The Brillouin zone for the body-centered cubic lattice is given in Fig. 1 and the symmetry axes and points labeled.

In order to determine the Fermi energy for the cubic phase the following procedure was adopted. We have from the definition of the density of states and the principles of Fermi statistics that

$$N/V=\int_0^{E_f}g(E)dE=(1/12\pi^3)\int k^3(E_F,\theta,\phi)d\Omega, \quad (6)$$

where N/V is the number of electrons/unit vol., $g(E)$ is the density of states, E_F is the Fermi energy, and k is the magnitude of the vector $\mathbf{k}$ for energy E_F and direction specified by θ and ϕ. The integral is over solid angle. This relation was used to determine the Fermi energy. In order to evaluate (6), we have expanded k^3 in terms of the Kubic harmonics[8] using the calculated values of k versus E from the energy bands along the three symmetry axes. A least-squares procedure was used to determine the coefficients. It was found that an accurate representation for the calculated values of k^3 versus E could be obtained from this procedure. Because the Kubic harmonics are orthogonal over the unit sphere, the only contribution to (6) comes from the spherically symmetric terms.

[8] F. C. Von der Lage and H. A. Bethe, Phys. Rev. **71**, 612 (1947).

The value obtained for the Fermi energy was then used to determine the values of the Fermi wave vector along the three symmetry axes by interpolation in the calculated energy-band data. In this manner an estimate of the distortion of the Fermi surface was obtained. Other methods could be used to determine the degree of anisotropy of the Fermi surface but for small distortions the direct method seems the most appropriate.

The effective mass was next determined from a similar expansion of the energy $E(k)$ in terms of the Kubic harmonics according to the expression

$$m^*=1/(E_2+2E_4k_f^2+3E_6k_f^4), \qquad (7)$$

where E_2, E_4, and E_6 are the coefficients of the spherical terms in the expansion of $E(\mathbf{k})$ versus $\mathbf{k}$. Because the Fermi surface is nearly spherical, the determination of the effective mass in this approximation which ignores anisotropic terms should be very nearly correct. We estimate that use of the spherical approximation produces an error of less than 0.01 in the effective mass.

In the calculation of the energy-band structure for the hexagonal phase of sodium we have taken the atomic volume to be the same as for the cubic phase. The values of the cell parameters quoted by Barrett[7] indicate that the volume per atom may be 0.2% larger for the hexagonal phase than for the cubic phase; however, the differences lie within the experimental error in the determination of the lattice constants. To within the experimental error, the c/a ratio is equal to 1.633 so that ideal close packing has been assumed.

The same pseudopotential has been employed and a sphere radius of 3.931 a.u. has been used. Energies are given in rydbergs and the same value of $V(0)$ is used except in comparing the Fermi energies for the two phases. For a comparison of the Fermi energies in the two phases, the shift in the average potential [which is $V(0)$] within the cellular polyhedron is taken into account. The evaluation of $V(0)$ for the two crystal structures is given in the Appendix.

The Brillouin zone for the hexagonal structure is given in Fig. 1 and the symmetry axes and symmetry points labeled. In performing the calculations for the hexagonal phase we have ignored spin-orbit coupling. In this case the energy levels along the hexagonal face of the Brillouin zone containing the points AHL are all doubly degenerate so that no gap will exist across the hexagonal face. The double-zone scheme is therefore applicable and we may continue the Δ_1 representation along the z axis through the first zone and into the second zone until the Fermi energy and Fermi surface are determined. Estimates[9] of the gap splitting that would be expected from spin-orbit coupling are of the order of 10^{-3} eV so that neglect of spin-orbit coupling in this calculation is probably justified. Even if the effect is not negligible, magnetic breakdown will occur for magnetic fields larger than about 30 Oe so that the "without spin-orbit" topology will be restored.[10]

[9] L. M. Falicov and M. H. Cohen, Phys. Rev. **130**, 92 (1963).

TABLE III. Energy eigenvalues for the Λ_1, Σ_1 and Δ_1 representations for body-centered cubic sodium.

x	$(ka/2\pi)$	First eigenvalue
Λ_1 Representation bcc lattice		
0.10	0.1732	−0.5879
0.20	0.3464	−0.5329
0.30	0.5196	−0.4416
0.40	0.6928	−0.3151
0.475	0.8227	−0.2007
Σ_1 Representation bcc lattice		
0.10	0.1414	−0.5940
0.20	0.2828	−0.5573
0.30	0.4242	−0.4963
0.40	0.5656	−0.4115
0.475	0.6717	−0.3343
Δ_1 Representation bcc lattice		
0.2	0.2	−0.5818
0.4	0.4	−0.5084
0.6	0.6	−0.3867
0.8	0.8	−0.2179
0.9	0.9	−0.1177

The energy-band calculation for the hexagonal phase employed a similar number of plane waves as was used for the cubic phase. The three symmetry axes T, Δ, and Σ and the symmetry points Γ and M were treated. Energies for the T_1, Δ_1, Σ_1, Σ_3, Σ_4, M_1^+, M_2^-, Γ_1^+, Γ_3^+, and Γ_4^- representations of predominantly s and p symmetry were determined.

The Fermi energy, degree of anisotropy of the Fermi surface, and the effective mass were determined in an analogous fashion to the procedure used for the cubic phase. Least-squares expansions were obtained using the hexagonal harmonics given by Bell[11] rather than the Kubic harmonics used for the cubic phase. It was found that accurate expansions in terms of the hexagonal harmonics were possible and the resulting band parameters such as the Fermi energy and the effective mass were found to change relatively little as the number of terms in the expansion was increased.

RESULTS

Table III contains the energies for states along the Λ, Σ, and Δ axes for the Λ_1, Σ_1, and Δ_1 representations, respectively. For the Λ axis, the coordinates of the $\mathbf{k}$ vector are given by $\mathbf{k}=(2\pi/a)(x,x,x)$ where $0<x<\frac{1}{2}$. The endpoints of this axis are the symmetry points Γ and P. Along the Σ axis, the coordinates of the k vector are given by $\mathbf{k}=(2\pi/a)(x,x,0)$ where $0<x<\frac{1}{2}$. The endpoints of this axis are the points Γ and N. The coordinates of the $\mathbf{k}$ vector along the Δ axis are given by $k=(2\pi/a)(x,0,0)$ where the $0<x<1$ and the endpoints are Γ and H.

[10] C. C. Grimes and A. F. Kip, Phys. Rev. **132**, 1991 (1963).
[11] D. G. Bell, Rev. Mod. Phys. **26**, 191 (1954).

TABLE IV. Energies for the Γ_1, N_1 and N_1' representations for the body-centered cubic sodium and the energy gap defined as $E(N_1')-E(N_1)$.

R_s	$E(\Gamma_1)$	$E(N_1)$	$E(N_1')$	E (Gap)
3.14511	−0.6537	−0.1185	−0.2335	−0.1150
3.83310	−0.6140	−0.2645	−0.3175	−0.0530
3.93139	−0.6062	−0.2758	−0.3223	−0.0465
4.02967	−0.5983	−0.2855	−0.3262	−0.0407
4.71767	−0.5434	−0.3256	−0.3339	−0.0083

Table IV contains the results for the Γ_1 representation and for the N_1 and N_1' representations. The energy gap at the point N defined as $E(N_1')-E(N_1)$ is also given. It is seen that the states N_1 and N_1' lie close together over a wide range of lattice spacings. For a sphere radius of 3.931 a.u. we obtain a gap at the point N of −0.0465 Ry. We obtain a value of the Fermi energy of −0.3724 Ry for the cellular zero of energy.[12] The spherical effective mass is found to be 1.024, and the distortion of the Fermi surface corresponds to a variation of the Fermi wave vector of approximately 0.2% with the bulge being in the direction of the point N. The results for the distortion of the Fermi surface and approach of the Fermi surface to the zone boundaries are contained in Table V.

The interband edge for direct transitions is estimated from the separation of the first and second eigenvalues for the Σ_1 representation evaluated at the Fermi surface

TABLE V. Distortion of the Fermi surface and approach of the Fermi vector to the zone boundaries for the body-centered cubic lattice.

Axis	$(ka/2\pi)_f$	Distortion	End point	$k_f/k_{\text{end point}}$ (%)
Δ	0.6190		H	62
Σ	0.6204	≈0.2%	N	88
Λ	0.6192		P	72

and is found to be approximately 2.18 eV. The energy difference between the Fermi energy and the lowest symmetry point in the second zone (N_1) is 1.31 eV. This probably corresponds to the edge for indirect optical transitions. The width of the occupied portion of the bands is 3.18 eV.

Table VI contains the results for the T_1 representation. The magnitude of the **k** vector along the T axis is given by $k=(2\pi/a)(2x/3)$ where $0<x<1$. The endpoints of this axis are the symmetry points Γ and K. Table VII contains the energies for the Δ_1 representation. This symmetry axis has as its endpoints the points Γ and A. The magnitude of the k vector along this axis is given by $k=(2\pi/a)(ax/c)$ where $0<x<\frac{1}{2}$ defines that portion of the axis lying within the first Brillouin zone. The Fermi surface lies outside the first Brillouin zone so that x has been extended to the range $0<x<1$. The Fermi energy corresponds to a value of x approximately equal to 0.9. Table VIII contains the results for the Σ_1, Σ_3, and Σ_4 representations. The magnitude of the **k** vector lying along the Σ axis is given by $k=(2\pi/a)(2x/\sqrt{3})$ where $0<x<\frac{1}{2}$.

Table IX contains the results for the M_1^+ and M_2^- representations. Also given is the energy gap at the point M defined as $E(M_1^+)-E(M_2^-)$. The gap, when the standard sphere radius is used, is found to be −0.0236 Ry and is approximately one-half the gap for the point N in the cubic phase. The gap remains small for a wide range of lattice spacings. Also included in Table IX are the results for the representations at the Γ point. On comparing Table IX with Table IV we see that the energies of the ground state at Γ are very nearly equal for both phases over the range of lattice constants treated.

TABLE VI. Energies for the T_1 representation of the hexagonal structure.

T_1 Representation hcp lattice x	$(ka/2\pi)$	First eigenvalue
0.20	0.1333	−0.5922
0.40	0.2667	−0.5511
0.60	0.4000	−0.4828
0.80	0.5333	−0.3877
1.00	0.6667	−0.2674

From the expansion of k^3 in the hexagonal harmonics we obtain a value of the Fermi energy for the hexagonal phase of −0.3721 Ry using the cellular zero of energy. Table X contains the results for the distortion of the Fermi surface and the approach of the Fermi surface to the zone boundaries. A distortion of approximately 0.22 to 0.29% is indicated. A slight increase in distortion in the hexagonal phase results from the closer approach of the Fermi surface to the zone boundary more than making up for the somewhat decreased gap at the zone boundary.

We obtain for the effective mass on the Fermi surface in the hexagonal phase a value of $m^*=1.029$. Figure 2 contains a plot of the calculated energy bands along the three symmetry axes. The symmetry points Γ, A, M, and K are indicated.

TABLE VII. Energies for the Δ_1 representations of the hexagonal structure.

Δ_1 Representation hcp lattice x	$(ka/2\pi)$	First eigenvalue
0.20	0.1224	−0.5940
0.40	0.2449	−0.5594
0.60	0.3674	−0.5018
0.80	0.4899	−0.4217
1.00	0.6124	−0.3243

[12] By "cellular zero" we mean that we have used $V(0)=-3/R_s+3Q/B^2R_s^3$, which is a spherical average of the potential as given in Eq. (1).

TABLE VIII. Energies for the Σ_1, Σ_3 and Σ_4 representations for the hexagonal structure.

x	$(ka/2\pi)$	First eigenvalue
Σ_1 Representation hcp lattice		
0.10	0.1155	−0.5954
0.20	0.2309	−0.5646
0.30	0.3464	−0.5134
0.40	0.4619	−0.4419
0.50	0.5773	−0.3516
Σ_3 Representation hcp lattice		
0.00	0.0000	−0.3370
0.10	0.1155	−0.3266
0.20	0.2309	−0.2955
0.30	0.3464	−0.2435
0.40	0.4619	−0.1709
0.50	0.5773	−0.0786
Σ_4 Representation hcp lattice		
0.00	0.0000	+0.4032
0.10	0.1155	+0.3100
0.20	0.2309	+0.2373
0.30	0.3464	+0.1854
0.40	0.4619	+0.1543
0.50	0.5773	+0.1439

CONCLUSIONS AND COMPARISON WITH EXPERIMENT

The Fermi energy for the cellular zero has been found to be −0.3724 and −0.3721 Ry for the cubic and hexagonal phases, respectively. Taking into account the small shift in the average potential within the cellular polyhedron for the two different phases, the result for the hexagonal phase is lowered slightly to $E_f = -0.3723$ Ry. If we neglect a possible change in the bandwidth resulting from a small increase in atomic volume (an 0.2% increase was suggested by Barrett), we obtain Fermi energies of −0.3724 and −0.3723 Ry for the cubic and hexagonal phases, respectively. Four significant figures in the energies have been given for purposes of illustration only. The last significant figure is uncertain so that we would conclude that the Fermi energies are equal in both phases and equal to −0.372 Ry for a sphere radius of 3.931 a.u.

TABLE IX. Energies for M_1^+, M_2^- and the representations at Γ. The energy gap at the point M is defined as $E(M_1^+) - E(M_2^-)$.

R_s	$E(M_1^+)$	$E(M_2^-)$	E(gap)	$E(\Gamma_1^+)$	$E(\Gamma_3^+)$	$E(\Gamma_4^-)$
3.1415	−0.2862	−0.2084	−0.0778	−0.6499		
3.9314	−0.3575	−0.3339	−0.0236	−0.6059	−0.3360	−0.2770
4.030	−0.3600	−0.3405	−0.0195	−0.5980		
4.717	−0.3613	−0.3621	+0.0008	−0.5427		

The distortion of the Fermi surfaces for the two phases was found to be approximately 0.2 and from 0.22 to 0.29%, respectively, for the cubic and hexagonal phases. Within the accuracy of the band calculations these estimates of the distortions should probably be considered to be the same. For the cubic phase our value for the distortion may be compared with that of Heine and Abarenkov.[13] Using a screened-ion pseudopotential they obtained a value for the distortion between 0.10 and 0.45%.

Our values for the effective masses of the two phases are regarded as equal and between 1.02 and 1.03 in value. These values are in reasonable agreement with those of Ham who obtained an effective mass equal to 1.0.[14] On the basis of our calculations a single effective mass is to be expected from samples of sodium containing amounts of both phases of sodium.

Table XI contains a comparison of our results for Γ_1, N_1, and N_1' with those of Ham,[14] Schlosser and Marcus,[15] and Callaway.[3] Agreement between the various authors is good but not perfect. Our value for the Fermi energy E_f is in good agreement with Ham's value.

TABLE X. Distortion of the Fermi surface and approach of the Fermi vector to the zone boundaries for the hexagonal close-packed structure.

Axis	$(ka/2\pi)_f$	Distortion	End point	$k_f/k_{\text{end point}}$ (%)
Σ	0.5523		M	95
Δ	0.5535	0.22 to 0.29%	A	180
T	0.5519		K	83

Our calculations have predicted a single effective mass for both phases of sodium. This prediction appears to be consistent with the cyclotron resonance work of Grimes and Kip[10] who found a single isotropic effective mass of 1.24 for sodium. The specific-heat measurements of Martin,[16] however, suggested that the effective masses in the two phases are substantially different. His measurements indicate that the thermal effective mass for the cubic phase of sodium is approximately 20% greater than for the hexagonal phase. Taking the experimental value of 1.27 for the effective mass of a sample containing approximately equal amounts of the two phases, the thermal effective mass for the cubic phase might be as large as 1.4.

TABLE XI. Comparative energy values for Na at a few symmetry points, from Ham, Schlosser and Marcus, Callaway and this paper.

	E (Ham)[a]	E (Schlosser and Marcus)[b]	E (Callaway)[c]	E (This paper)[d]
Γ_1	−0.6041	−0.6067	−0.5974	−0.60625
N_1	−0.2910	−0.2944	−0.263	−0.2758
N_1'	−0.3078	−0.2938	−0.316	−0.3223
E_f	−0.369			−0.3724

[a] F. S. Ham (Ref. 13). A lattice constant of 8.11 a.u. was used.
[b] H. Schlosser and P. M. Marcus, Ref. 14. A lattice constant of 8.0427 a.u. was used.
[c] J. Callaway (Ref. 3).
[d] A lattice constant equal to 7.984 a.u. was employed.

[13] V. Heine and I. Abarenkov, Phil. Mag. **9**, 451 (1964).

[14] F. S. Ham, Phys. Rev. **128**, 82, 2524 (1962).
[15] H. Schlosser and P. M. Marcus, Phys. Rev. **131**, 2529 (1963).
[16] D. L. Martin, Phys. Rev. **124**, 438 (1961).

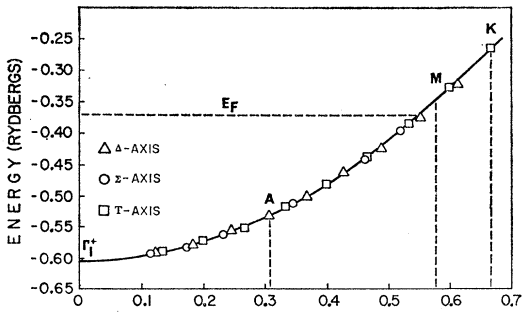

FIG. 2. Calculated energy bands along the Σ, Δ, and T symmetry axes for hexagonal close-packed sodium.

Hodgson[17] has recently measured the optical constants of sodium in the wavelength range from 0.65 to 2.5 μ. His infrared measurements indicate an optical mass of 1.08 ± 0.01. A somewhat lower value for the optical effective mass was given by Cohen[18] who analyzed the data of Ives and Briggs[19] and found $m^*_{op}=1.01\pm0.02$.

Hodgson's results for the conductivity indicate an interband edge at about 1.2 eV which is probably an indirect transition. This is in reasonable agreement with our value 1.3 eV if the transition connects the Fermi surface with the symmetry point N_1.

APPENDIX: FOURIER COEFFICIENTS OF THE POTENTIAL

The crystal potential is taken to be a superposition of potentials

$$V(r)=-2/r+Qe^{-Br}/r, \tag{A1}$$

located at each atom site of the crystal. The potential is neutralized by a uniform charge distribution within the cellular polyhedron. The Fourier coefficients of the crystal potential can be determined taking full account of the symmetry of the cellular polyhedron most easily through a consideration of the charge distribution which produces the Coulombic portion of the crystal potential.

By expanding both the potential and the charge distribution in terms of reciprocal lattice vectors and applying Poisson's equation, we obtain

$$V(\mathbf{k})=-(8\pi/N\Omega_0\mathbf{k}^2)\int\rho(\mathbf{r})\exp[-i\mathbf{k}\cdot\mathbf{r}]d^3r, \tag{A2}$$

where the integral is over the crystal containing N cellular polyhedra of volume Ω_0. Since the charge distribution $\rho(r)$ has the symmetry of the lattice, (A2) may be written as

$$V(\mathbf{k})=(8\pi/\Omega_0\mathbf{k}^2)\int\rho(\mathbf{r})\exp[-i\mathbf{k}\cdot\mathbf{r}]d^3r, \tag{A3}$$

where the integral is over one cellular polyhedron.

We next evaluate the Fourier coefficients of the potential for the body-centered cubic lattice. The first term in (A1) represents a lattice of point charges. Therefore inserting a delta function charge distribution into (A3) we obtain for the Coulombic portion of the Fourier coefficients of the potential

$$V(k)_{\text{Coul.}}=-8\pi/\Omega_0\mathbf{k}^2. \tag{A4}$$

Because the second term in (A1) arises out of the orthogonality requirement between valence and core-electron wave functions rather than from an electrostatic distribution of charge, we shall evaluate the Fourier coefficients for this term directly. Writing the potential as a sum over lattice sites

$$V(\mathbf{r})_{\text{rep}}=\sum_m Q\exp-B|\mathbf{r}-\mathbf{r}_m|/|\mathbf{r}-\mathbf{r}_m|. \tag{A5}$$

The Fourier coefficients for this term are then given by

$$V(\mathbf{k})=(Q/N\Omega_0)\sum_m\int\exp[-i\mathbf{k}\cdot\mathbf{r}]\times\exp-B|\mathbf{r}-\mathbf{r}_m|/|\mathbf{r}-\mathbf{r}_m|d^3r, \tag{A6}$$

where the integral is over all space and the sum is over all lattice sites. Integrating and performing the sum, we obtain for the repulsive portion

$$V(\mathbf{k})_{\text{rep}}=+4\pi Q/[\Omega_0(k^2+B^2)]. \tag{A7}$$

The uniform charge distribution contributes only to the average potential $V(0)$ so that for $k\neq0$, the Fourier coefficients of the potential are

$$V(\mathbf{k})=-(4\pi/\Omega_0\mathbf{k}^2)[2-(Q\mathbf{k}^2/B^2+\mathbf{k}^2)]. \tag{A8}$$

The average potential $V(0)$ will be considered separately.

In evaluating the Fourier coefficients of the potential for the hexagonal structure, the above procedures are again applicable provided the integrations are taken over the double cellular polyhedron containing the two atoms of the basis. We obtain for the Fourier coefficients of the potential (for $k\neq0$) for the hexagonal structure

$$V(\mathbf{k})=\tfrac{1}{2}[\exp(-i\mathbf{k}\cdot\mathbf{r}_1)+\exp(-i\mathbf{k}\cdot\mathbf{r}_2)]V(|\mathbf{k}|), \tag{A9}$$

where

$$V(|\mathbf{k}|)=-(4\pi/\Omega_0k^2)[2-Qk^2/(B^2+k^2)]. \tag{A10}$$

The reciprocal lattice vectors k here of course relate to hexagonal lattice. The radius vectors $\mathbf{r}_1$ and $\mathbf{r}_2$ are from the origin to the two atoms of the basis.

We next consider the average crystal potential $V(0)$. The contribution due to the repulsive potential is obtained immediately from (A7). We shall consider the contribution arising from the uniform charge distribution within the cellular polyhedron next since the point charges do not contribute to the average po-

[17] J. N. Hodgson, Phys. Chem. Solids 24, 1213 (1963).
[18] M. H. Cohen, Phil. Mag. 3, 762 (1958).
[19] H. E. Ives and H. B. Briggs, J. Opt. Soc. Am. 27, 181 (1937).

tential. Callaway and Glasser[20] have given $V(0)$ due to the uniform charge distribution for the cubic lattice, and we have calculated $V(0)$ for the hexagonal lattice. The results are given below:

$$V(0)_{\text{hcp}} = -(4\pi/\Omega_0)0.06250 a_{\text{hcp}}^2,$$
$$V(0)_{\text{bcc}} = -(4\pi/\Omega_0)0.0495536 a_{\text{bcc}}^2, \quad \text{(A11)}$$

where a_{hcp} and a_{bcc} are the lattice constants for the two lattices. Taking the atomic volumes to be the same in both the hexagonal and cubic phases and referring both results to the same lattice constant, we obtain a numerical comparison for $V(0)$ for both phases.

$$V(0)_{\text{hcp}} = -(4\pi/\Omega_0)0.0496063 a_{\text{bcc}}^2,$$
$$V(0)_{\text{bcc}} = -(4\pi/\Omega_0)0.0495536 a_{\text{bcc}}^2. \quad \text{(A12)}$$

While $V(0)_{\text{hcp}}$ is slightly more binding than $V(0)_{\text{bcc}}$, the differences are quite small.

[20] J. Callaway and M. L. Glasser, Phys. Rev. **112**, 73 (1958).

PHYSICAL REVIEW VOLUME 136, NUMBER 5A 30 NOVEMBER 1964

Boltzmann Equation in a Phonon System*

C. Horie† and J. A. Krumhansl
Laboratory of Atomic and Solid State Physics, Cornell University, Ithaca, New York
(Received 10 July 1964)

The Green's function approach is developed to derive the Boltzmann equation for a phonon system having cubic anharmonic interactions. Within the framework of the lowest order scattering process, it is found that the steady-state Boltzmann equation obtained is identical with the Peierls integral equation, except for small correction terms. These correction terms can be absorbed into the transport term by replacing the phonon group velocity appearing in the transport term by the renormalized one, including kinetic and dynamical effects of collisions. Several remarks are made on the generalization of the Boltzmann equation.

I. INTRODUCTION

In this paper, we derive the Boltzmann equation for the phonon distribution only, in a crystal which is subject to a constant and small thermal disturbance such as a temperature gradient and in which phonons interact only with each other through a cubic anharmonic interaction.

Within the framework of the approximation in which only the lowest order scattering process is retained, we can find that the Peierls integral equation[1] for a phonon distribution is to be modified by correction terms. These terms are related to the spatial variation of the phonon distribution, so that they can be interpreted as renormalizing the phonon group velocity in the transport term of the Peierls equation.

The derivation of the Boltzmann equation is carried out here by means of the Green's function method. Kadanoff and Baym[2] have developed the Green's function approach to derive the Boltzmann equation for particle systems of either fermions or bosons subject to a mechanical disturbance. We proceeded initially along similar lines. In the particle case, there are certain difficulties concerning the choice of the boundary conditions for the Green's function defined in a real time domain. However, the thermodynamical Green's function defined for imaginary times satisfies definite boundary conditions. Then, using the relationship between the real-time and the imaginary-time Green's functions, and converting the equation of motion for the imaginary-time Green's function into that for the real-time Green's function, the Boltzmann equation for a particle distribution function results. Thus, the essential part of this derivation of the Boltzmann equation appears to rest on the unique relationship between the real-time and the imaginary-time Green's functions; and this, in turn, is determined by the assumptions imposed on the asymptotic behavior of the system at the time $t=-\infty$ at which the mechanical disturbance was turned on adiabatically.

On the other hand, in the present case of phonons, we have a rather different situation in several respects. First, in addition to the wave nature of phonons, the cubic anharmonic interactions do not conserve the number of phonons. Second, the external disturbance applied to the system is not a mechanical one. To cope with this situation, we have had to use arguments rather different from those used in the particle case.

In Sec. II, we introduce a "nonequilibrium" phonon Green's function D, which is defined by the statistical average of the complex time correlation of "displacement" operators. This nonequilibrium phonon Green's function is different from the usual definition of a phonon Green's function in that no specific functional form is assumed for the density matrix specifying the

* Work supported by the U. S. Atomic Energy Commission.
† Permanent address: Department of Physics, Tohoku University, Sendai, Japan.
[1] R. E. Peierls, *Quantum Theory of Solids* (Oxford University Press, Oxford, 1955).
[2] L. P. Kadanoff and G. Baym, *Quantum Statistical Mechanics* (W. A. Benjamin, Inc., New York, 1962).